An Optimal Networked LiFi Access Point Slicing Scheme for Internet-of-Things

Hamada Alshaer and Harald Haas
LiFi R&D centre, Technology & Innovation Centre
The University of Strathclyde, UK
{h.alshaer,h.haas}@strath.ac.uk

Oluwatayo Y. Kolawole
School of Engineering
The University of Edinburgh, UK
O.Kolawole@ed.ac.uk

***Abstract*—Light-Fidelity (LiFi) access points (APs) can be deployed anywhere to support the exponential growth of various lightweight hand-held and smart internet-of-things (IoT) devices and applications. IoT traffic is often sporadic and consists of heterogeneous bursty flows, which may affect the performance of supported wireless services. This paper develops an optimal data rate-based slicing scheme that dynamically virtualizes a networked LiFi AP downlink channel bandwidth according to the data rate demands of users and the requested services. We formulate a game optimization problem that captures the relation between three main entities: a LiFi attocellular network infrastructure provider (InP), mobile virtual network operators (MVNOs), and IoT or wireless users. A software-defined networking (SDN) controller enables the InP to reconfigure the LiFi AP downlink channel slices to MVNOs, based on their service-level agreements (SLAs) and the traffic profile of IoT services. Simulation results show that the proposed AP resources slicing scheme is promising for IoT applications.**

***Index Terms*—LiFi networks virtualization, LiFi AP slicing, Internet-of-Things, matching game theory.**

I. Introduction

Light-Fidelity (LiFi) attocellular networks can be deployed wherever functional light bulbs provide illumination [1]. A networked LiFi access point (AP) represents an ideal wireless access point of presence to support internet-of-things (IoT) devices and applications. These are expected to form a major portion of the fifth generation (5G) mobile wireless networks, which have diverse communication patterns and generate sporadic traffic with short packet lengths [2]. The legacy one-size-fits-all architectures cannot meet the heterogeneous quality-of-service (QoS) requirements of services in 5G networks [3]. An efficient and flexible network architecture is thus required to reprogram resource allocation to IoT and other wireless applications in accordance with their utilization and service requirements.

An architecture is proposed, which integrates software-defined networking (SDN) and data distribution service (DDS) middleware [4], [5], as depicted in Fig. 1. An SDN controller programs the allocation of virtualized resources to the different mobile virtual network operators (MVNOs), while the DDS middleware can guarantee reliable and real-time data exchange for the IoT applications [6]. A LiFi attocellular network infrastructure provider (InP) can share resources at the network level or at the AP downlink channel bandwidth (ADCB) level. In essence, a LiFi attocell AP is a small optical wireless cell

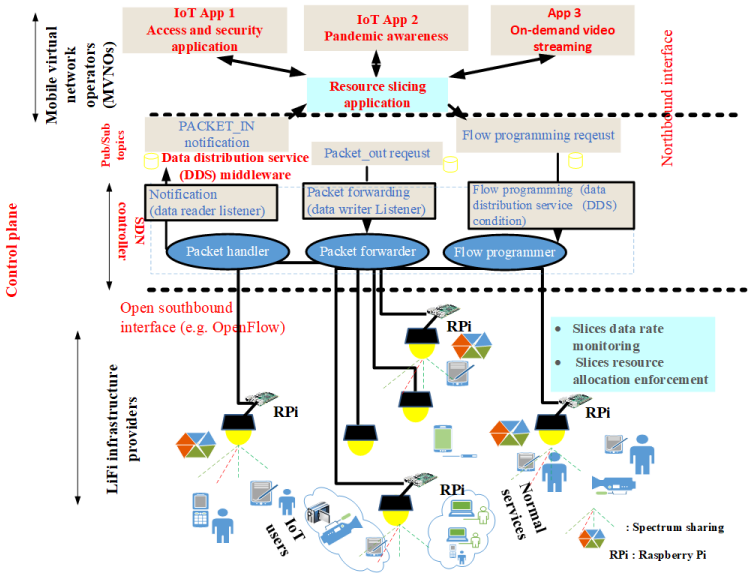

Fig. 1: SDN-enabled LiFi attocellular network virtualization.

that can be allocated as a whole to a single MVNO at the network level, while only having its channel bandwidth shared among MVNOs at the AP level. On either level, the LiFi attocellular network can be virtualized via resource or rate-based provisioning [7], [8].

A resource-based provisioning scheme is developed in [7], which dynamically allocates the LiFi ADCB as sets of resource blocks to slices. In contrast, within the proposed architecture shown in Fig. 1, this paper develops a rate-based provisioning optimization scheme for slicing the LiFi AP downlink channel resource, which guarantees adaptive data rates per slice while ensuring an effective data rate per user. While the users are subscribed to the different MVNOs, the proposed scheme dynamically allocates the resources that effectively meet the data rate requirements of MVNOs and their users. Dynamic slicing approaches are also developed for on-demand cloud radio access network in [3], [9], [10]. Whereas our proposed scheme underlines the operations of an application that should run on the northbound of the SDN controller to support the creation of LiFi AP downlink channel slices for on demand IoT and other wireless applications.

A sliced LiFi ADCB is part of a large virtualized indoor network topology deployed in an airport to support appli-

This is a peer-reviewed, accepted author manuscript of the following article: Alshaer, H., Haas, H., & Kolawole, O. Y. (2021). An optimal networked LiFi access point slicing scheme for internet-of-things. In 2021 IEEE International Conference on Communications Workshops (ICC Workshops) IEEE. https://doi.org/10.1109/iccworkshops50388.2021.9473868

cations ranging from video on demand (VoD) streaming to IoT security and pandemic awareness, as shown in Fig. 1. In this use case, we designate the LiFi APs, located near the gates (ingress/egress), as edge APs, with the remaining being allocated as core APs. While the downlink channel bandwidth of edge APs is shared among the MVNOs at the AP level, the core LiFi APs are shared at the network level. As part of a successful virtualization for a whole LiFi attocellular network, we focus on slicing a networked LiFi ADCB among MVNOs. The main actors in the LiFi attocellular network virtualization are a LiFi network InP, MVNOs, and IoT devices or mobile wireless users. The relation among these players is formulated in an optimization design scheme that considers LiFi ADCB resource parameters, minimum data rate requirement per user, and the type and number of user traffic requests.

The rest of this paper is structured as follows. In Section II, we describe our system and LiFi ADCB resource models. Section III formulates the sliced LiFi ADCB as a dynamic utility optimization problem for the InP and MVNOs. In Section IV, a matching game theory-based heuristic scheme is proposed to solve the optimization problem and provide some analysis on convergence. Section V discusses the performance evaluation of the proposed heuristic scheme. Finally, Section VI summarizes the main conclusion and findings.

II. System Model

This system model is proposed to dynamically share an indoor LiFi attocellular network among a number of MVNOs. Edge (ingress or egress) APs have their own centralized Raspberry Pi (RPi) to process some information relating to local bandwidth resource slicing in coordination with the SDN controller that manages the LiFi attocellular network, as shown in Fig. 1. An orthogonal frequency-division multiple access (OFDMA) scheme manages the LiFi ADCB in the network. The LiFi AP channel bandwidth, W, is represented by a set of $\mathcal{S} \triangleq \{1, \ldots, s, \ldots, S\}$ orthogonal sub-channels (sub-carriers). The LiFi AP uses half of these sub-carriers to realize the Hermitian conjugate of the complex-valued symbol after modulation, as only real-valued signals can be transmitted to users.

The LiFi ADCB resources are virtualized through description, discovery and composition processes which enable the LiFi network InP to share them among a set of $\mathcal{N} \triangleq \{1, \ldots, n, \ldots, N\}$ MVNOs. A MVNO, n, can serve M_n users according to their pre-defined service level agreement (SLA). The users include IoT and other multimedia wireless devices that are LiFi enabled. A sub-channel resource, s, which is allocated to user m receiving services from MVNO n provides data rate based on the capacity lower bound [11], given by

$$R^s_{n,m} = \frac{1}{2} b_s \log\left(1 + c\frac{\Gamma_{n,m} p_{n,m} h^2_{n,m}}{\sum_{t\in\mathcal{N}, t\neq n} \Gamma_{t,m} p_{t,m} h^2_{t,m} + \sigma^2_m}\right), \tag{1}$$

where $p_{t,m}$ denotes the inter-MVNOs interference power that user m receives from a neighbouring AP providing services to MVNO t on the same sub-channel s. b_s denotes the bandwidth of sub-channel s; c denotes a constant, defined as $c = e/2\pi$, with e as Euler's constant; $\Gamma_{n,m}$ and $p_{n,m}$ denote the user's responsivity and received optical power of user m with MVNO n, respectively; and $h_{n,m}$ represents the channel gain between the AP and user m with MVNO n. Similarly, $\Gamma_{t,m}$, $p_{t,m}$ and $h_{t,m}$ are the corresponding values for user m with MVNO t; and σ^2_m denotes the variance of zero-mean additive white Gaussian noise that consists of both shot and thermal noises. The channel gain, $h_{n,m}$, combines both line-of-sight (LoS) and non-line-of-sight (NLoS) characteristics of the optical wireless channel, given by

$$h_{n,m} = h^{\text{LoS}}_{n,m} + h^{\text{NLoS}}_{n,m}. \tag{2}$$

Here, $h^{\text{LoS}}_{n,m}$ is defined as the direct current (DC) gain of the direct link between the user m and the AP. It follows the Lambertian emission pattern, given as [12]

$$h^{\text{LoS}}_{n,m} = \begin{cases} \nu \frac{k+1}{2\pi} \cos^k(\vartheta) \frac{A_m}{d^2_{nm}} \cos(\psi) g_f g(\psi), & 0 \leq \psi \leq \Psi_c \\ 0, & \psi > \Psi_c, \end{cases} \tag{3}$$

where ν denotes the blocking factor, indicating whether the AP and LiFi dongle photo detector (PD) are within their field of views (FoVs). k denotes the Lambert index, a measure of the directional characteristics of the AP, which is related to the half power semi-angle of the AP, $\phi_{1/2}$, given as

$$k = \frac{-\ln 2}{\ln(\cos\phi_{1/2})}. \tag{4}$$

Note that ϑ and ψ represent the angle of radiance with respect to the normal axis ($\mathbf{n_t}$) of the AP and the angle of incidence with respect to the normal axis ($\mathbf{n_r}$) of the PD, respectively; Ψ_c denotes the PD's FoV; g_f denotes the gain of the optical filter; and $g(\psi)$ denotes the optical concentrator gain given as

$$g(\psi_)) = \begin{cases} \frac{\zeta^2}{\sin^2\Psi_c}, & 0 \leq \psi \leq \Psi_c \\ 0, & \psi > \Psi_c. \end{cases} \tag{5}$$

Here, ζ denotes the refractive index; A_R and $\mathrm{d}_{T,R}$ denote the PD's physical area and the distance between the transmitter and receiver's PD, respectively.

On the other hand, $h^{\text{NLoS}}_{n,m}$ is the DC gain of the NLoS link, which includes all the multiple reflections of the transmitted signal. It is assumed that a discrete reflector model divides the walls, floor and ceiling of an indoor environment into small reflective surfaces [13]. If a wall is segmented into Q surface elements, then h^{NLoS}_{nm} can be given by

$$h^{\text{NLoS}}_{n,m} = \mathbf{r}^T \mathbf{G}_\eta \left(\mathbf{I} - \mathbf{H}_s \mathbf{G}_\eta\right)^{-1} \mathbf{t}, \tag{6}$$

where $\mathbf{r} = [H_{m,1}, H_{m,2} \ldots H_{m,Q}]^T$ denotes the transfer function from all Q reflective elements to the user m. The entries of $\mathbf{r}$ are modelled as Lambertian radiators with the Lambert index, $k = 1$, and given as

$$H_{m,a} = \frac{\nu_{m,a} A_m}{\pi d^2_{m,a}} \cos\left(\vartheta_{m,a}\right) \cos\left(\psi_{m,a}\right), \forall a \in [1, Q], \tag{7}$$

where $\nu_{m,a}$ and $d_{m,a}$ are the visibility factor and Euclidean distance between the ath reflective surface and user m, respectively; and $\vartheta_{m,a}$ and $\psi_{m,a}$ denote the corresponding angles of radiance and incidence with respect to their normal vectors, respectively. Similarly, $\mathbf{t} = [H_{1,T}, H_{2,T} \dots H_{Q,T}]^T$ denotes the transfer vector from the AP to all reflective surfaces with entries given as

$$H_{b,T} = \frac{\nu_{b,T} A_b}{\pi d_{b,T}^2} \cos(\vartheta_{b,T}) \cos(\psi_{b,T}), \ \forall b \in [1, Q]. \quad (8)$$

Here, A_b represents the area of the bth reflective surface and the variable definitions of $\nu_{b,T}$, $d_{b,T}, \vartheta_{b,T}, \psi_{b,T}$ follow those specified for (7). The matrix $\mathbf{H}_s \in \mathbb{C}^{Q \times Q}$ denotes the transfer function describing the LoS links between all reflective surfaces in the room; $\mathbf{I} \in \mathbb{C}^{Q \times Q}$ and $\mathbf{G}_\eta = \text{diag}(\eta_1, \eta_2, \dots, \eta_Q)$ are the identity and reflectivity matrices, respectively. Note that $\eta_i \in [0, 1]$, is a factor that measures the reflectance efficiency of the ith surface [13]. Users receive different data rates according to the sub-channels allocated to them based on (1). Let $\rho^s_{n,m}$ be a binary variable, which equals 1 if a user m of MVNO n is allocated a sub-channel s; and 0 otherwise. MVNO n, $\forall n \in \mathcal{N}$, aims to maximize the transmitted data rate of their users while minimizing the price of their InP slice resources, as defined by the following utility function:

$$u_n(\boldsymbol{\rho}, c^b_n) = \sum_{m \in M_n} \sum_{s \in \mathcal{S}} c^b_n R^s_{n,m} - \sum_{s \in \mathcal{S}} c^s_n \sum_{m \in M_n} \rho^s_{n,m}, \quad (9)$$

where $R^s_{n,m}$ is defined in (1); and c^s_n and c^b_n are the price that InP charges MVNO n per sub-channel s and MVNOs charge users per bps, respectively. Meanwhile, the utility function of the InP aims to maximize the number of utilized resources, as defined by

$$u_I(\boldsymbol{\rho}, \mathbf{c}) = \sum_{n \in \mathcal{N}} \rho_n c^s_n, \quad (10)$$

where $\rho_n = \sum_{m \in M_n} \sum_{s \in \mathcal{S}} \rho^s_{n,m}$ denotes the total number of sub-channels allocated to MVNO n to serve their users M_n.

III. Problem Formulation

Our formulated optimization problem of the LiFi ADCB slicing aims to maximize the utility functions (10) and (9) of the InP and MVNOs, subject to ensuring intra-AP slice isolation and meeting data rate per user requirement, as defined by

$$\max_{\mathbf{c}, \boldsymbol{\rho}} \quad u_I(\boldsymbol{\rho}, \boldsymbol{c}) + \sum_{n \in \mathcal{N}} u_n(\boldsymbol{\rho}, c^b_n) \quad (11a)$$

$$\text{s.t.} \sum_{n \in \mathcal{N}} \sum_{m \in M} \rho^s_{n,m} \leq |\mathcal{S}| \quad (11b)$$

$$\sum_{m \in M} \omega_{n,m} r^{\max}_{n,m} \leq \sum_{m \in M} \sum_{s \in \mathcal{S}} R^s_{n,m}, \ \forall n \quad (11c)$$

$$\sum_{s \in \mathcal{S}} \sum_{n \in \mathcal{N}} \rho^s_{n,m} \leq 1, \ \ \forall m \quad (11d)$$

$$\rho^s_{n,m} \in \{0, 1\} \ \ , \forall n, m, s \quad (11e)$$

$$c^s_n, c^b_n \in [c_{\min}, c_{\max}], \ \forall n, s \quad (11f)$$

where $\omega_{n,m} \in [0, 1]$, $\forall n, m$, is a weight parameter by which the SDN controller can program resource allocation in accordance with the data rate SLA per InP-MVNO, and MVNO n and user m. The controller can also enable the InP and MVNOs to dynamically adjust their prices, c^s_i, c^b_n, of the slice resources and data rate in bps offered to the MVNOs and users, respectively. This provides competitive data rates to the different users while maximizing the InP revenue and MVNOs profit. The total allocated sub-channels to the MVNOs should not exceed what the InP can provide per (11c). Also, the total data rate offered to the users of MVNOs should not exceed what can be achieved by their total slice resources per (11d). A user can be subscribed to a single MVNO per (11d), which reduces interference among MVNOs per AP in the network. The price of sub-channels, c^s_i, is determined according to the demands of MVNOs. Similarly, the price of data rate, c^b_n, offered to the users is determined according to their demand and traffic profile per (11f). While the MVNOs can provide up to the maximum data rate to their users, the weight $\omega_{n,m}$ can be optimally set to values that better match the different data rates of users. This can enable the MVNOs to guarantee a minimum data rate to their users.

IV. Heuristic data-rate based slicing scheme

The InP and MVNOs have different utility functions, requiring both to act independently in order to maximize their utility subject to mutual resource constraints and service requirements, as expressed in (11a). For practical considerations, Matching game theory is used to provide an ideal framework to solve research problems that involve independent actors and distributed decision makers [14], which we integrate in our proposed scheme to solve the LiFi ADCB slicing optimization problem (11a)–(11f). The InP and MVNOs-users are the actors in this game, in which each aims to maximize their utility functions while efficiently meeting the data rate requirements of the different users subscribed with the MVNOs.

A. Matching concepts and procedure

The relationship between the InP and MVNOs-users is managed through a matching procedure, which has been developed using the college admission model [15]. Users are mapped as the students and the AP downlink sub-channels are mapped as the colleges. Each user (student) subscribed to the MVNOs can access a single sub-channel of the AP (college) which can serve multiple users. The preferences of users and sub-channels are designed in terms of data rate, price and MVNO. The InP starts by exchanging some information with the MVNOs, namely data rate and the price of each sub-channel. The users exchange, with MVNOs, their data rate and price per bps demands. This exchanged information enables a user m to choose a MVNO n and build a preference list, $L_{n,m}$, based on the data rate and price information of sub-channels exchanged with the InP. The preference list ranks the sub-channels in descending order with regards to their price and the difference between their achievable data rate and requested data rate based on (12). Subsequently, the MVNO n chooses

Algorithm 1: Heuristic matching game algorithm

1 **Input**: $r_s \ \forall s \in \mathcal{S}$ and $r_{n,m}^{\min} = \omega_{n,m} r_{n,m}^{\max}, \quad \forall n, m$
2 Number of unmatched users: $L_u = NM_n$
3 **for** *MVNO* $n \in \mathcal{N}$ **do**
4 **for** *user* $m \in \mathcal{M}$ **do**
5 Compute $L_{n,m}$ from (12)
6 **end**
7 **end**
8 **for** *sub-channel* $s \in \mathcal{S}$ **do**
9 Compute L_s from (IV-A) and $r_{n,m}^{\min}$
10 **end**
11 **while** $L_u \neq 0$ **do**
12 **for** *MVNO* $n \in \mathcal{N}$ **do**
13 **for** *user* $m \in \mathcal{M}$ **do**
14 **if** $L_{n,m}$ *is not empty* **then**
15 user m requests and then removes his best matched resource in $L_{n,m}$
16 **end**
17 **end**
18 **end**
19 **for** *sub-channel* $s \in \mathcal{S}$ **do**
20 **if** *users requests match their preference in* L_s **then**
21 all users requests are assigned their preferred resource
22 **else**
23 only $|\mathcal{W}_s|$ users are assigned to resource s and the rest are rejected
24 **end**
25 Update L_u, as $L_u = L_u - |\mathcal{W}_s|$
26 **end**
27 **end**

for his user m the top-ranked sub-channel that better matches his price and data rate demand.

$$\max \left(R_{n,m}^{s} - r_{n,m}^{\min} \right), \ \forall s \in \mathcal{S}, \tag{12}$$

where $r_{n,m}^{\min} = \omega_{n,m} r_{n,m}^{\max}$ represents the minimum data rate requirement of user m with MVNO n.

On the other hand, the InP dynamically prices the sub-channels according to their utilization by the users of MVNOs. Hence, the matching procedure maps the users to the sub-channels that maximize their utilization. For each sub-channel, s, the slicing scheme ranks a preferred subset, $\mathcal{W}_s$ of users with the MVNOs, which meets their data rate and price requirements. The highest ranked subset of users for the sub-channel, s, is determined based on the satisfaction of $\max \left\{ |\mathcal{W}_s| : R_{\mathcal{W}_s}^{s} - r_{\mathcal{W}_s}^{\min} \right\}$, where $\mathcal{W}_s \subseteq \bigcup_{n \in \mathcal{N}} M_n$, $R_{\mathcal{W}_s}^{s}$ denotes the sum rate of all users in $\mathcal{W}_s$, and $|\mathcal{W}_s|$ represents the cardinality of subset $\mathcal{W}_s$.

Our proposed heuristic matching procedure uses the achievable data rate and price of sub-channels and data rate requirements of users with MVNOs to pair them, as outlined in Algorithm 1. The matching process starts by unmatching all users, as indicated in step 1. The preference lists for each user, $L_{n,m}$, and each sub-channel list, L_s, are created in steps $3-10$. Then, the algorithm runs a number of iterations to map the users to their best ranked sub-channel choice. It processes the requests per sub-channel, while checking that the users match in the preferred subset $\mathcal{W}_s$. If there is a match, the sub-channel s is allocated to all requesting users in steps $19--24$. The iterations continue until all the users are matched with their corresponding sub-channels, where $L_u = 0$. A stable matching is defined as optimal when every user experiences at least the same quality of service with the current match as it would with any other stable matching. The iterative process of the sub-channels mapping to the MVNOs-users in Algorithm 1 converges to a stable optimal assignment. From step 5, resource s is ranked higher than resource s' in the preference list of user m. This implies that at step 15, user m requests the first resource s. If at the end of process, user m is allocated resource s', this implies that resource s is already matched with users ranked higher in their preference lists than user m, following steps 20-23. This leaves no bandwidth for user m to deviate from the current matching. At each iteration, users delete the preferred resource from their lists after making a request in step 15, which makes algorithm 1 a variant of the deferred acceptance method [16]. The algorithm achieves a convergence with an optimal solution, when the users to sub-channels matching process becomes stable.

TABLE I: Simulation Parameters

Notation	Parameter	Values
$\phi_{1/2}$	LED half power semi angle	60°
η_w	Reflectivity factor of wall	0.8
g_f	Gain of optical filter	1
A_R	Physical area of PD	10 mm^2
η_f	Reflectivity factor of floor	0.8
N_0	Noise power spectral density	$10^{-}21$ A^2/Hz
B	Modulated bandwidth	20 MHz
h	Height of the light	3 m
η_c	Reflectivity factor of ceiling	0.8
N_{sub}	Number of sub-channels	128
D	Number of active sub-channels	63
Ψ_c	Receiver FOV	90°
P_t	Transmission power	8.8W
ζ	Refractive index	1.5
$\mathbf{n_r}$	PD's orientation vector	[0, 0, 1]
R_{PD}	PD responsivity	0.5 A/W
$\mathbf{n_t}$	AP's orientation vector	[0, 0, -1]
$\mathcal{S}$	DCO-OFDM subcarriers	128

V. Performance Evaluation

A discrete time simulation environment was developed in MATLAB to evaluate the performance of our proposed heuristic data-rate based slicing algorithm 1. We consider a LiFi attocellular network composed of 6 LiFi APs, in which 4 APs are placed at the edge and two at the centre, as shown in 1. This network provides services to users uniformly distributed in a room of size $8 \times 6 \times 4$ ($L \times W \times H$). The LiFi APs' parameters in the network are summarized in Table I [17]. There are three

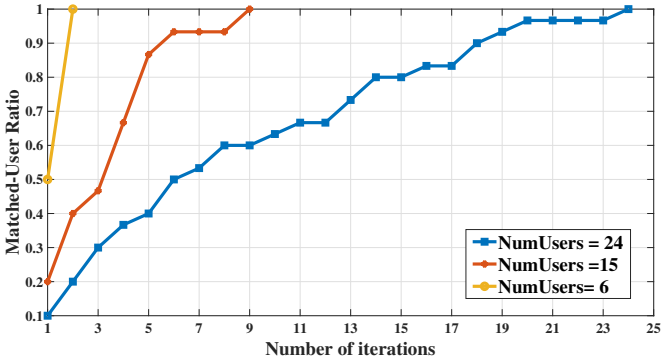

Fig. 2: Convergence of Algorithm 1 for varying numbers of user requests.

MVNOs that share the edge LiFi ADCB in the SDN-enabled network shown in Fig. 1. Each MVNO has a maximum and minimum data rate SLA with the LiFi InP, which offers their users a minimum data rate, $r_{n,m}^{\min} = \omega_{n,m} r_{n,m}^{\max}$. The respective traffic flows of IoT and the multimedia services of users are generated with data rates following a Poisson distribution with λ taken to 64 kbps–1 Mbps and a Pareto distribution with a scale parameter taken to $0.5 - -2$ Mbps [3], [7].

Our performance analysis starts by illustrating the evolution of the matching game algorithm 1 in Fig. 2. The user requests are generated with an equal minimum data rate of 1 Mbps for all MVNOs. The matched-user request ratio is computed per iteration by dividing the number of matched user requests to sub-channels by the total requests of users. The matching algorithm converges to a stable solution, where all the requests of users are matched in $2, 9$ and 24 iterations when the total number of user requests are $6, 15$ and 30 respectively, as shown in Fig. 2. The steady segments shown in Fig. 2 depict situations where the user requests are rejected by the slicing scheme because of mismatching, with the preference profile of sub-channels at steps 19–23. Nevertheless, in the three scenarios, the users requests are matched in fewer iterations than the total users requests, demonstrating the viability of our proposed matching scheme for LiFi ADCB.

While the MVNOs guarantee a minimum data rate for their users, the InP should meet the SLA requirements of services that run on different LiFi ADCB slices. This scenario analyses the capability of matching algorithm 1 to meet the SLA average delay and acceptance rate of the IoT traffic generated from user requests with MVNOs 1,3 and VoD service requests generated from users with MVNO 2. The average delay is calculated as the average of the elapsed times between the transmission and reception times of the packets transmitted to all users per MVNO, considering the bandwidth of their resources allocated to users on the downlink channel. The average acceptance rate is computed at the end of the algorithm iterations by dividing the total number of matched user requests to sub-channels by the total users requests subscribed to a MVNO. We observe from Fig. 3 that, despite the increase in the IoT user requests from 10 to 15,

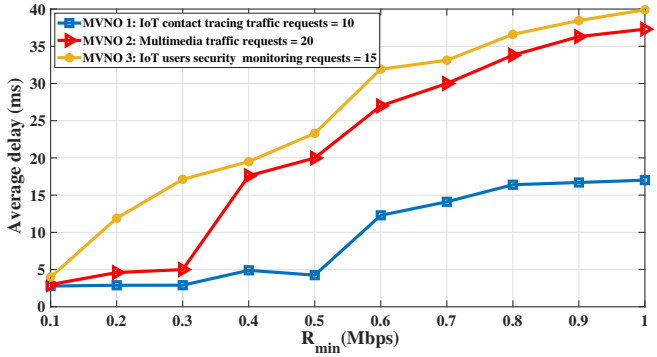

(a)

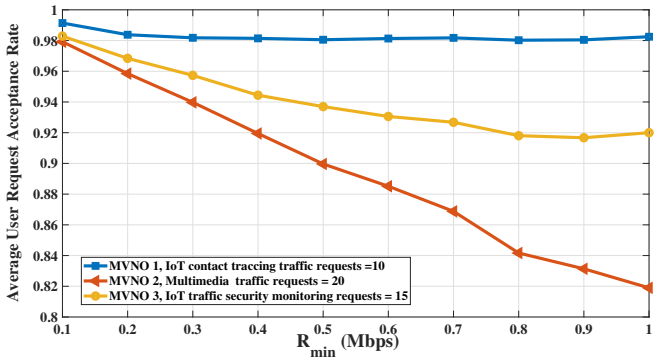

(b)

Fig. 3: (a) Average delay per MVNO. (b) Acceptance rate per MVNO with respect to minimum rate requirements.

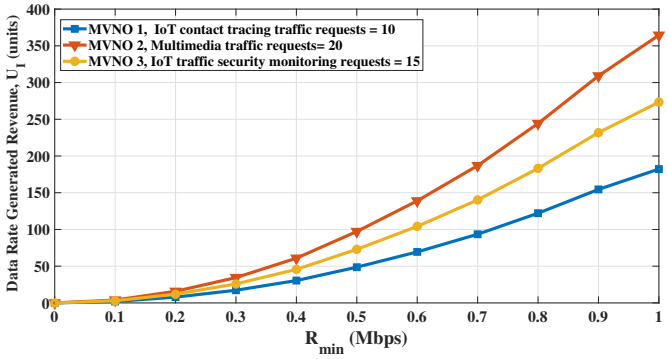

Fig. 4: Data rate generated revenue for LiFi network InP.

the acceptance rate and average delay were maintained within reasonable bounds. Additionally, we observe a higher delay for multimedia user requests compared to IoT users requests, as shown in Fig. 3a. This can be explained by the fact that when the number of users requests increases, they experience a drop in their acceptance rate because the full slice resource utility is reached. Nevertheless, the proposed matching game algorithm 1 could achieve over 80% acceptance rate for the MVNO_2 with a higher user request demand while meeting their SLA requirements, as shown in Fig. 3a,b.

Fig. 4 depicts the evaluation of InP utility (i.e. revenue) obtained from the different MVNOs subleasing channel bandwidth from their LiFi APs. As an example, we set the price

of 2 units per 100 kbps data rate provided to each MVNO. The InP revenue from each MVNO is calculated based on (10). The result from the different MVNOs is then compared based on their data rate requirements. Fig. 4 shows that the InP revenue depends mainly on the user requests acceptance rates and their data rate. For example, MVNO 3 pays 280 units for its services when requiring a minimum of 15 Mbps, whereas the data rate requirement of 9 Mbps costs only 108 units.

Finally, the scenario illustrated by Fig. 5 evaluates the capability of the matching algorithm 1 to achieve inter-slice isolation and slicing flexibility in the resource allocation per slice based on the MVNOs data rate requirements. Accordingly, it is shown that the matching algorithm 1 achieves the maximum throughput of each MVNO. The unutilized resources of some MVNOs are allocated to others requiring more throughput. In Fig. 5, the total throughput of MVNOs are measured while changing the traffic load of their slices over the simulation time. With a change in the MVNO traffic load every 20 s, it can be seen that in the first 20 s, MVNOs 1,2,3 could achieve their maximum total throughput per slice, which are approximately 10 Mbps, 15 Mbps and 20 Mbps, respectively, as shown in Fig. 5. Then, in the second and third 20 s, it is shown that the total throughput of MVNOs changes according to the data rate requirements of their users.

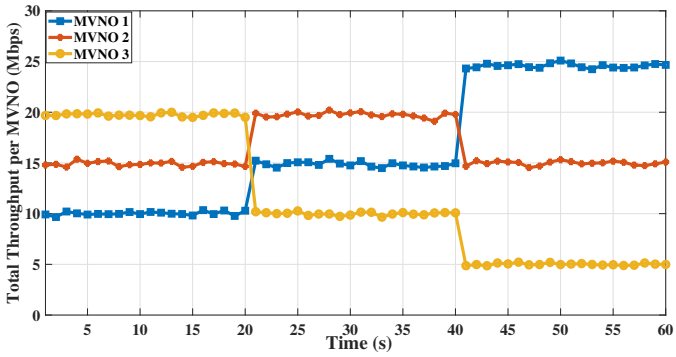

Fig. 5: MVNOs throughput versus simulation time.

VI. Conclusion

This paper introduced a DDS and SDN-enabled LiFi attocellular network architecture to support IoT and other wireless applications that generate different traffic patterns with heterogeneous QoS requirements. It also supports the control and management of virtualized resources in LiFi attocellular networks. In essence, this paper has applied a matching game algorithm to manage the LiFi ADCB slices allocation to MVNOs according to their data rate requirements and generated traffic load. We observed that the matching game theory can lead to a stable relationship between different players having various interests in sharing the LiFi attocell AP downlink channel bandwidth. We have found out that the InP could achieve better revenue from MVNOs with higher data rate requirements, even with a small number of users. The MVNOs with a larger number of users requesting small data rates consumes more resources which results in a reduction of the InP revenue. The SDN controller enabled the InP and MVNOs to adjust the resource allocation and the sublease, according to the user traffic profile and data rate demand. This demonstrates the viability of our proposed SDN-based network slicing solution to ensure flexible LiFi ADCB sharing between multiple MVNOs, while ensuring inter-slice isolation. This work enables us to develop customized wireless resource slicing schemes that can better support the emerging real-time applications relating to healthcare and security.

Acknowledgment

This work was supported by the EPSRC under grants EP/L020009/1 (TOUCAN Project), H2020-ICT-2019 5G-CLARITY project, and EP/R007101/1 (Established Career Fellowship), as well as by the Wolfson Foundation and the Royal Society.

References

[1] H. Haas, "High-speed wireless networking using visible light," *SPIE Newsroom*, April 2013.

[2] W. Ejaz, A. Anpalagn, M. A. Imran *et al.*, "Internet of Things (IoT) in 5G Wireless Communications," *IEEE Access*, vol. 4, pp. 10 310–10 314, September 2016.

[3] S. Costanzo, I. Fajjari, N. Aitsaadi, and R. Langar, "Dynamic Network Slicing for 5G IoT and eMBB services: A New Design with Prototype and Implementation Results," in *Proc. of the 3rd Cloudification of the Internet of Things (CIoT)*, January 2018.

[4] J. Kim and J. W. Lee, "OpenIoT: An Open Service Framework for the Internet of Things," in *Proc. of the IEEE World Forum on Internet of Things (WF-IoT)*, March 2014, pp. 89–93.

[5] Object Management Group, "Data-Distribution Service for Real-Time Systems," *OMG Version 1.4*, September 2014.

[6] A. Hakiri, P. Berthou, A. Gokhale, and S. Abdellatif, "Publish/Subscribe-Enabled Software-defined networking for efficient and scalable IoT Communications," *IEEE Communication magazine*, pp. 48–54, September 2015.

[7] H. Alshaer and H. Haas, "Bidirectional LiFi attocell access point slicing scheme," *IEEE Transactions on Network and Service Management*, vol. 15, no. 3, pp. 909–922, September 2018.

[8] J. S. Panchal, R. D. Yates, and M. M. Buddhikot, "Mobile Network Resource Sharing Options: Performance Comparisons," *IEEE Trans. on Wireless Comm.*, vol. 12, no. 9, pp. 4470–4482, September 2013.

[9] K. Samdanis, X. C. Perez, and V. Sciancalepore, "From Network Sharing to Multi-Tenancy: The 5G Network Slice Broker," *IEEE Communication Magazine*, vol. 54, pp. 32–39, July 2016.

[10] S. D'Oro, F. Restuccia, A. Talamonti, and T. Melodia, "Typhoon: An SDN enhanced real-time big data streaming framework," in *Proc. of IEEE Conference on Computer Communications (INFOCOM)*, Paris, France, June 2019, pp. 310–322.

[11] R. Jiang, Q. Wang, H. Haas, and Z. Wang, "Joint user association and power allocation for cell-free visible light communication networks," *IEEE Journal on Selected Areas in Communications*, vol. 36, no. 1, pp. 136–148, 2018.

[12] J. M. Kahn and J. R. Barry, "Wireless infrared communications," *Proceedings of the IEEE*, vol. 85, no. 2, pp. 265–298, Feb 1997.

[13] H. Schulze, "Frequency-domain simulation of the indoor wireless optical communication channel," *IEEE Transactions on Communications*, vol. 64, no. 6, pp. 2551–2562, June 2016.

[14] Z. Han, D. Niyato, W. Saad, T. Başar, and A. Hjørungnes, *Game theory in wireless and communication networks: theory, models, and applications*. Cambridge university press, 2012.

[15] D. Gale and L. Shapley, "College admissions and the stability of marriage," *The American Mathematical Monthly*, vol. 69, no. 1, pp. 9–15, 1962.

[16] A. E. Roth, "Deferred acceptance algorithms: History, theory, practice, and open questions," *international Journal of game Theory*, vol. 36, no. 3-4, pp. 537–569, 2008.

[17] D. Tsonev, S. Sinanovic, and H. Haas, "Practical MIMO Capacity for Indoor Optical Wireless Communication with White LEDs," in *Proc. of IEEE VTC-Spring*, June 2013.